

**NASA TECHNICAL
MEMORANDUM**

NASA TM X-62,425

NASA TM X-62,425

(NASA-TM-X-62425) AN APPROXIMATE
CLOSED-FORM SOLUTION FOR LEAD LAG DAMPING OF
ROTOR BLADES IN HOVER (NASA) 27 p HC \$3.75
CSCL 01A

N75-22276

**G3/02 Unclass
20749**

**AN APPROXIMATE CLOSED-FORM SOLUTION FOR LEAD-LAG
DAMPING OF ROTOR BLADES IN HOVER**

David A. Peters

**Ames Research Center
and**

**U. S. Army Air Mobility R&D Laboratory
Moffett Field, Calif. 94035**



April 1975

1. Report No. TM X-62,425	2. Government Accession No.	3. Recipient's Catalog No.	
4. Title and Subtitle AN APPROXIMATE CLOSED-FORM SOLUTION FOR LEAD-LAG DAMPING OF ROTOR BLADES IN HOVER		5. Report Date	
		6. Performing Organization Code	
7. Author(s) David A. Peters		8. Performing Organization Report No. A-6025	
		10. Work Unit No.	
9. Performing Organization Name and Address Ames Research Center and U.S. Army Air Mobility R&D Laboratory Moffett Field, Calif., 94035		11. Contract or Grant No.	
		13. Type of Report and Period Covered Technical Memorandum	
12. Sponsoring Agency Name and Address National Aeronautics and Space Administration Washington, D. C. 20546		14. Sponsoring Agency Code	
		15. Supplementary Notes	
16. Abstract Simple stability methods are used to derive an approximate, closed-form expression for the lead-lag damping of rotor blades in hover. Destabilizing terms are shown to be a result of two dynamic mechanisms. First, the destabilizing aerodynamic forces that can occur when blade lift is higher than a critical value are maximized when the blade motion is in a straight line equidistant from the blade chord and the average direction of the air flow velocity. This condition occurs when the Coriolis terms vanish and when the elastic coupling terms align the blade motion with this least stable direction. Second, the nonconservative stiffness terms that result from pitch-flap or pitch-lag coupling can add or subtract energy from the system depending upon whether the motion of the blade tip is clockwise or counterclockwise.			
17. Key Words (Suggested by Author(s)) Helicopter Rotor blade		18. Distribution Statement Unclassified - Unlimited STAR Category 02	
19. Security Classif. (of this report) Unclassified	20. Security Classif. (of this page) Unclassified	21. No. of Pages 27	22. Price* \$3.75

AN APPROXIMATE CLOSED-FORM SOLUTION FOR LEAD-LAG

DAMPING OF ROTOR BLADES IN HOVER

David A. Peters

U. S. Army Air Mobility R&D Laboratory
and
Ames Research Center

SUMMARY

Simple stability methods are used to derive an approximate, closed-form expression for the lead-lag damping of rotor blades in hover. Destabilizing terms are shown to be a result of two dynamic mechanisms. First, the destabilizing aerodynamic forces that can occur when blade lift is higher than a critical value are maximized when the blade motion is in a straight line equidistant from the blade chord and the average direction of the air flow velocity. This condition occurs when the Coriolis terms vanish and when the elastic coupling terms align the blade motion with this least stable direction. Second, the nonconservative stiffness terms that result from pitch-flap or pitch-lag coupling can add or subtract energy from the system depending upon whether the motion of the blade tip is clockwise or counterclockwise.

INTRODUCTION

Flap-lag stability is an important fundamental basis for the study of hingeless rotorcraft dynamics. Although a simple flap-lag analysis is not adequate for the absolute determination of blade stability, it is invaluable for giving insight into the basic physical mechanisms that underly the more complex dynamic phenomena. Reference 1 described the flap-lag dynamics of a hingeless rotor in hover by using the simplified model of a rigid blade with root spring restraint. Numerical results provided a systematic study of the effect of blade parameters on rotor stability, and applications of Routh's criteria identified stability boundaries for some specialized conditions. The present paper studies this same problem using different methods that provide additional explanations of the system behavior. These methods permit the development of an approximate, closed-form expression for the lead-lag damping. In addition, the methods illustrate the specific contributions of various dynamic mechanisms to the blade damping.

SYMBOLS

a	lift curve slope per radian
C_{d_0}	profile drag coefficient
[C]	matrix coefficients of $\dot{\beta}, \dot{\zeta}$ terms
[D]	damping matrix, $\frac{1}{2} [C + C^T]$
F_1, F_2	dimensionless elastic forces
[G]	Coriolis matrix, $\frac{1}{2} [C - C^T]$
i	$\sqrt{-1}$
[K]	stiffness matrix
p	rotating flapping frequency divided by Ω
\bar{p}	equivalent flapping frequency, $\sqrt{p^2 - \frac{\gamma}{8} \theta_\beta}$
R	elastic coupling parameter
s	Laplace transform variable, rad^{-1}
x_1, x_2	flap and lead-lag directions
β	perturbation flapping angle, positive up, rad
β_0	equilibrium flapping angle, rad
β_{pc}	precone angle, rad
γ	Lock number
δ	angle between lead-lag direction and the principal axis of blade motion, rad
δ_m	angle between lead-lag direction and the direction of the natural vibrations of the rotating blade in a vacuum, $\frac{\Delta}{\omega_\zeta^2 - p^2}$, rad
$\bar{\delta}_m$	modified δ_m including pitch-flap and pitch-lag coupling, $\frac{\Delta - \frac{\gamma}{8} \theta_\zeta}{\omega_\zeta^2 - \bar{p}^2}$
$\delta\theta$	perturbation pitch angle, $\theta_\beta \beta + \theta_\zeta \zeta$, rad
Δ	elastic coupling term

$\Delta\theta$	partial derivative of Δ , $\frac{\partial\Delta}{\partial\theta}$
ϵ	perturbation of lead-lag eigenvalue, rad^{-1}
ζ	perturbation lead-lag angle, positive forward, rad
ζ_0	equilibrium lead-lag angle, rad
η	real portion of ϵ , rad^{-1}
θ	equilibrium pitch angle, $\theta_0 + \theta_\beta(\beta_0 - \beta_{pc})$, rad
θ_0	collective pitch, rad
$\theta_\beta, \theta_\zeta$	pitch-flap and pitch-lag coupling
$\bar{\theta}_\beta$	coupling due to θ_β , $\left[\phi + \frac{\delta}{\gamma}(\beta_0 - \beta_{pc})\Delta\theta\right]\theta_\beta$
λ	eigenvalue of [D]
$\begin{Bmatrix} \lambda \\ \beta \\ \zeta \end{Bmatrix}$	eigenvector of [D]
ρ	thickness ratio of ellipse of motion (positive for clockwise motion)
ϕ	average inflow angle (A of ref. 1), rad
ϕ_β	flapping component of lead-lag mode shape when lead-lag component = 1, $\phi_\beta = \delta + i\rho$
ω_ζ	lead-lag frequency divided by Ω
Ω	rotor rotational speed, rad^{-1}
$(\dot{\quad})$	$\frac{d}{d(\Omega t)}$
$(\quad)^*$	complex conjugate

BACKGROUND

The linearized flap-lag equations of motion, as derived in reference 1, may be written in the form

$$\begin{Bmatrix} \ddot{\beta} \\ \ddot{\zeta} \end{Bmatrix} + \begin{bmatrix} C_{11} & C_{12} \\ C_{21} & C_{22} \end{bmatrix} \begin{Bmatrix} \dot{\beta} \\ \dot{\zeta} \end{Bmatrix} + \begin{bmatrix} K_{11} & K_{12} \\ K_{21} & K_{22} \end{bmatrix} \begin{Bmatrix} \beta \\ \zeta \end{Bmatrix} = \begin{Bmatrix} 0 \\ 0 \end{Bmatrix} \quad (1)$$

where

$$C_{11} = \frac{\gamma}{8}$$

$$C_{12} = 2\beta_0 - \frac{\gamma}{8} (2\theta - \phi)$$

$$C_{21} = -2\beta_0 + \frac{\gamma}{8} (\theta - 2\phi)$$

$$C_{22} = \frac{\gamma}{8} \left(2 \frac{C_{d0}}{a} + \theta\phi \right)$$

$$K_{11} = p^2 - \frac{\gamma}{8} \theta_{\beta} \equiv \bar{p}^2$$

$$K_{12} = \Delta - \frac{\gamma}{8} \theta_{\zeta}$$

$$K_{21} = \Delta + \left[\frac{\gamma}{8} \phi + (\beta_0 - \beta_{pc}) \Delta_{\theta} \right] \theta_{\beta} \equiv \Delta + \frac{\gamma}{8} \bar{\theta}_{\beta}$$

$$K_{22} = \omega_{\zeta}^2$$

and β_0 , $\sqrt{\zeta_0}$, θ , ϕ , θ_{ζ} , $\bar{\theta}_{\beta}$, $\sqrt{C_{d0}/a}$ are considered small quantities whose products may be neglected with respect to unity. Equation (1) also contains a contribution from the homogeneous terms of reference 1, $(\beta_0 - \beta_{pc}) \Delta_{\theta} \theta_{\beta}$ in K_{21} , that results from the effect of pitch-flap coupling on the steady elastic pitch angle.

From reference 1, it is known that the least stable mode of motion is predominantly lead-lag. It is also known that the frequency of the motion is near ω_{ζ} and that the damping is very small. This allows a perturbation solution for equation (1) to be derived. The perturbation solution is obtained by applying the following perturbation expressions to the Laplace transformed equation (1).

$$\left. \begin{aligned} s &= i\sqrt{K_{22}} + \epsilon \\ \begin{pmatrix} \beta \\ \zeta \end{pmatrix} &= \begin{pmatrix} \phi_\beta \\ 1 \end{pmatrix} \end{aligned} \right\} \quad (2)$$

where ϵ and ϕ_β are considered small quantities.

$$\begin{bmatrix} K_{11} - K_{22} & K_{12} \\ +iC_{11}\sqrt{K_{22}} & +iC_{12}\sqrt{K_{22}} \\ K_{21} & iC_{22}\sqrt{K_{22}} \\ +iC_{21}\sqrt{K_{22}} & +2i\epsilon\sqrt{K_{22}} \end{bmatrix} \begin{pmatrix} \phi_\beta \\ 1 \end{pmatrix} = \begin{pmatrix} 0 \\ 0 \end{pmatrix} \quad (3)$$

The solution of equation (3) is simply

$$\epsilon = -\frac{C_{22}}{2} + \frac{[K_{12} + iC_{12}\sqrt{K_{22}}][K_{21}i - C_{21}\sqrt{K_{22}}]}{2\sqrt{K_{22}}(K_{22} - K_{11} - iC_{11}\sqrt{K_{22}})} \quad (4a)$$

$$\phi_\beta = \frac{K_{12} + iC_{12}\sqrt{K_{22}}}{(K_{22} - K_{11}) - iC_{11}\sqrt{K_{22}}} \quad (4b)$$

Equations (4a) and (4b) give the change in frequency $\text{Im}(\epsilon)$, damping $\text{Re}(\epsilon)$, and mode shape θ_β due to the presence of flap-lag coupling. They imply that transient motion of the blade tip is a slowly decaying or growing ellipse. Although equation (4a) can be directly applied to obtain an approximate expression for lead-lag damping, the identical result can be obtained by applying simple stability methods to equation (1). This latter method has the advantage of describing the specific contributions of various dynamic mechanisms to the blade damping and will be used in this paper.

NEGATIVE AERODYNAMIC DAMPING

The first stability method to be considered is based on the Kelvin-Tait-Chetaev theorem, reference 2. This theorem applies to equation (1) when no pitch-flap or pitch-lag coupling is present ($\theta_\beta = \theta_\zeta = 0$) and when the matrix [C] is decomposed into symmetric and antisymmetric parts.

$$[D] \equiv \frac{1}{2} [C + C^T] \quad \text{damping matrix}$$

$$[G] \equiv \frac{1}{2} [C - C^T] \quad \text{Coriolis matrix}$$

The theorem states that if [D] has all positive eigenvalues, then the system is stable if, and only if, [K] has all positive eigenvalues. Stated another way, the theorem implies that if [K] has all positive eigenvalues, then a necessary, but not sufficient, condition for instability is that [D] have a negative eigenvalue. Thus, for a hingeless rotor without pitch coupling, for which [K] is always positive definite, an instability can occur only if [D] has a negative eigenvalue. The Coriolis and stiffness terms are conservative and can provide no positive or negative damping of their own.

Therefore, the stability of equation (1) is determined by the eigenvalues of the damping matrix

$$[D] = \frac{\gamma}{8} \begin{bmatrix} 1 & -\frac{\theta + \phi}{2} \\ -\frac{\theta + \phi}{2} & \theta\phi + 2\frac{C_{d0}}{a} \end{bmatrix} \quad (5)$$

One can obtain approximate values for the eigenvalues of [D] by utilizing the fact that ϕ , θ , C_{d0}/a are small quantities. The eigenvalue λ and eigenvector $\langle \lambda_\beta, \lambda_\zeta \rangle$ are given from

$$\begin{bmatrix} \frac{\gamma}{8} - \lambda & -\frac{\gamma}{16}(\theta + \phi) \\ -\frac{\gamma}{16}(\theta + \phi) & \frac{\gamma}{8}\left(\theta\phi + 2\frac{C_{d0}}{a}\right) - \lambda \end{bmatrix} \begin{Bmatrix} \lambda_\beta \\ \lambda_\zeta \end{Bmatrix} = \begin{Bmatrix} 0 \\ 0 \end{Bmatrix}$$

and are

$$\lambda = \frac{\gamma}{8}, \quad \frac{\gamma}{8} \left[2\frac{C_{d0}}{a} - \frac{(\theta - \phi)^2}{4} \right] \quad (6a)$$

$$\begin{Bmatrix} \lambda_\beta \\ \lambda_\zeta \end{Bmatrix} = \begin{Bmatrix} 1 \\ -\frac{\theta + \phi}{2} \end{Bmatrix}, \quad \begin{Bmatrix} \frac{\theta + \phi}{2} \\ 1 \end{Bmatrix} \quad (6b)$$

The term $\theta - \phi$ in the smaller lead-lag mode eigenvalue is the average blade angle of attack. Thus, the lead-lag damping decreases quadratically with the blade lift. Blade instabilities are only possible when the eigenvalue becomes negative and creates a source of negative damping. This can occur when the blade lift exceeds the critical value.

$$(\theta - \phi) > 2\sqrt{2 \frac{C_{d0}}{a}} \quad (7)$$

This relation was also derived in reference (1) by application of Routh's criteria.

The corresponding eigenvector of [D], equation (6b), shows that this minimum value of damping occurs along an axis which is equidistant from the blade chord line and the direction of the mean air flow velocity relative to the blade. Thus, there exists an axis of minimum damping that makes an angle $(\theta + \phi)/2$ with the lead-lag direction, as shown in figure 1. Blade motions nearly aligned with this axis will be unstable when equation (7) is fulfilled, but motions deviating from this axis will be stabilized by the large flap damping that exists in the direction perpendicular to the $(\theta + \phi)/2$ axis.

Another way of looking at this phenomenon is to consider the aerodynamic forces when blade motions make an angle δ with the lead-lag direction, figure 1. Blade motion in the positive lead-lag direction with $\delta = 0$ increases the blade lift, but the lift has a component in the negative lead-lag direction. Therefore, the increased lift opposes the motion and provides damping. For blade motions with $\phi < \delta < \theta$, the lift is similarly increased by positive velocities. In this case, however, the lift has a component in the positive direction of motion and therefore adds energy to the motion providing negative damping. When $\delta > \theta$, the lift is decreased by positive lead-lag velocity and the motion is stabilized. The aerodynamic energy added to the blade is maximum when $\delta = (\theta + \phi)/2$. The fact that the minimum damping occurs along the $(\theta + \phi)/2$ axis can also be derived by calculating the work done on the blade by the aerodynamic forces and showing that this energy is maximized when $\delta = (\theta + \phi)/2$. The relation between the direction of motion and the damping (or energy dissipation) is illustrated in figure 2 where the damping coefficient in the direction of blade motion is plotted versus δ . The minimum damping (i.e., the eigenvalue) occurs at the midpoint of the destabilizing region. Flap-lag instabilities in hover are a result of this negative aerodynamic damping.

In the previous discussion, the blade was assumed to move in a straight line. The blade may actually move, however, around an elliptical path as shown in figure 3. Thus, even when the principal axis of motion is along the $(\theta + \phi)/2$ axis, blade motions can be in the flap direction near the tips of the ellipse. This flap motion will stabilize the blade by introducing flap damping into the system. Since the uncoupled flap damping $\gamma/8$ is nearly an order of magnitude larger than the uncoupled lead-lag damping, $(\gamma/8)[(2C_{d0}/a) + \theta\phi]$, flapping motion is highly stabilizing. For blade elliptical motion with thickness ratio ρ and tilted from the lead-lag plane by an angle δ , the flapping component of the mode shape is

$$\phi_B = \delta + i\rho \quad (8)$$

where δ and ρ are assumed small. The generalized damping of this mode is determined in the same manner as is the generalized mass or stiffness: the damping matrix is pre- and post-multiplied by the mode shape.

$$-2\eta = \langle \phi_\beta \quad 1 \rangle [D] \begin{Bmatrix} \phi_\beta \\ 1 \end{Bmatrix}^* \quad (9a)$$

$$\eta = \frac{\gamma}{16} \left[-2 \frac{C_{d0}}{a} + \frac{(\theta - \phi)^2}{4} \right] - \frac{\gamma}{16} \left[\left(\delta - \frac{\theta + \phi}{2} \right)^2 + \rho^2 \right] \quad (9b)$$

The parameter η is the real portion of the eigenvalue. The first bracketed term in equation (9b) is the negative damping from the portion of the motion parallel to the $(\theta + \phi)/2$ axis. The second term is the positive flap damping obtained from the portion of the motion perpendicular to the $(\theta + \phi)/2$ axis. Equation (9b) gives the quantitative effect of mode shape on lead-lag damping. Motions along the $(\theta + \phi)/2$ axis are least stable, and deviations from this axis (either in angle or ellipse thickness ratio) stabilize the motion by utilizing the large flap damping.

ELASTIC COUPLING

The previous discussion implies that coupling between flap and lead-lag motion will be destabilizing if it tends to align blade motions with the $(\theta + \phi)/2$ axis. One effect that can produce such a coupling is the amount of elastic (structural) coupling between flap and lead-lag. This effect is represented mathematically by the off-diagonal terms of the stiffness matrix. For small pitch angles, the stiffness matrix of the spring model in reference 1 may be approximated by

$$[K] = \begin{bmatrix} p^2 & \Delta \\ \Delta & \omega_\zeta^2 \end{bmatrix} \quad (10)$$

where

$$\left. \begin{aligned} \Delta &\approx R\theta(\omega_\zeta^2 - p^2 + 1) \\ 0 &\leq R \leq 1 \end{aligned} \right\} \quad (11)$$

and R is an elastic coupling parameter. For this discussion Δ need not be restricted to this form, and in a later section the effects of pitch-flap and pitch-lag coupling on the stiffness matrix will be considered.

Because of the elastic coupling Δ , the natural vibrations for the blade rotating in a vacuum will be inclined with respect to the lead-lag plane by an angle δ_m , as shown in figure 4. For small Δ and $\omega_\zeta \neq p$, this angle is given by

$$\delta_m = \frac{\Delta}{\omega_\zeta^2 - p^2} \quad (12)$$

The inclination of the mode in a vacuum δ_m is not generally equivalent to the inclination of the mode including aerodynamics δ . For the special case of $\delta_m = (\theta + \phi)/2$ and $[G] = 0$, however, aerodynamic coupling is eliminated and δ does equal δ_m . Thus, the least stable condition occurs when δ and δ_m are aligned with the $(\theta + \phi)/2$ axis

$$\Delta|_{\text{least stable}} = \frac{(\omega_\zeta^2 - p^2)(\theta + \phi)}{2} \quad (13)$$

For example, the least stable condition for the approximation in equation (11) is

$$R|_{\text{least stable}} = \frac{\left(1 + \frac{\phi}{\theta}\right)(\omega_\zeta^2 - p^2)}{2(\omega_\zeta^2 - p^2 + 1)} \quad (14)$$

A similar result that was obtained in reference 1 from Routh's criteria, is that the smallest $(\theta - \phi)$ for instability occurs when equation (14) is satisfied.

A quantitative expression for the relation between elastic coupling and blade damping can be obtained by applying the mode shape component ϕ_β , equation (4b), to the damping expression in equation (9b). Assuming again that $[G] = 0$, ϕ_β is given by

$$\phi_\beta = \delta + ip = \frac{\theta + \phi}{2} + \frac{\left[\Delta - \frac{\theta + \phi}{2}(\omega_\zeta^2 - p^2)\right]}{(\omega_\zeta^2 - p^2)^2 + \left(\frac{\gamma}{8}\omega_\zeta\right)^2} \left[(\omega_\zeta^2 - p^2) + i\frac{\gamma}{8}\omega_\zeta\right] \quad (15)$$

Equation (15) shows that an inclination of the modal axis δ_m with respect to the $(\theta + \phi)/2$ axis results in elliptical blade motions. An expression for the lead-lag damping can be obtained by substituting equation (15) into equation (9b).

$$-\frac{16}{\gamma}\eta = 2\frac{C_{d0}}{a} - \frac{(\theta - \phi)^2}{4} + \frac{\left[\Delta - \frac{\theta + \phi}{2}(\omega_\zeta^2 - p^2)\right]^2}{(\omega_\zeta^2 - p^2)^2 + \left(\frac{\gamma}{8}\omega_\zeta\right)^2} \quad (16)$$

Equation (16) contains two components of damping: (1) the minimal possible damping $2(C_{d0}/a) - (\theta - \phi)^2/4$, and (2) the stabilizing effect of separating the δ_m axis and the $(\theta + \phi)/2$ axis. Equation (16) also shows that above or below certain critical values of Δ (or δ_m) no instability is possible. The blade motion is always stable when

$$\left| \frac{\Delta}{\omega_\zeta^2 - p^2} - \frac{\theta + \phi}{2} \right| > \frac{\theta - \phi}{2} \sqrt{1 + \left(\frac{\frac{\gamma}{8}\omega_\zeta}{\omega_\zeta^2 - p^2}\right)^2}$$

This is illustrated in figure 5 which indicates regions of possible instability when $p = \sqrt{4/3}$, $\gamma = 8$. Instabilities are only possible when the modal axis δ_m is sufficiently close to the $(\theta + \phi)/2$ axis, and the least stable condition occurs when $\delta_m = (\theta + \phi)/2$. At $\omega_\zeta = p$, the definition for δ_m breaks down and instabilities appear to be possible at all values of δ_m . In terms of Δ at $\omega_\zeta = p$, however, instabilities are only possible when

$$|\Delta| < \frac{\gamma}{16} (\theta - \phi) \omega_\zeta$$

The least stable condition occurs when $\Delta = 0$.

Also shown in figure 5 are lines of constant R in the $\delta_m, \omega_\zeta^2 - p^2$ plane. For $\phi/\theta < R < 1$, instabilities can only occur when ω_ζ is above a critical value. For R values in the upper half of this region, $[1 + (\phi/\theta)]/2 < R < 1$, the least stable condition $\delta_m = (\theta + \phi)/2$ is never obtained; but in the lower half of the region, $\phi/\theta < R < [1 + (\phi/\theta)]/2$, the least stable condition is obtained for some finite value of ω_ζ . For $R < \phi/\theta$, instabilities can only occur when ω_ζ lies between upper and lower critical values.

When $\theta + \phi$ and $\theta - \phi$ are positive, which is the case for hover or axial flight, instabilities are not possible for sufficiently soft inplane rotors with $0 < R < 1$. Blade motion is always stable when

$$p^2 - \omega_\zeta^2 > \frac{\gamma}{16} \omega_\zeta \frac{\theta - \phi}{\sqrt{\theta\phi}}$$

Thus, most physically realistic soft inplane configurations are stable in hover. When $\theta + \phi$ is negative, however, such as is the case in autorotation conditions, the stability boundaries in figure 5 will move down with respect to the constant R contours; and potential instabilities can occur for some realistic soft inplane configurations, $\omega_\zeta < p$.

CORIOLIS COUPLING

Another effect that can couple flap and lead-lag motion is the Coriolis matrix $[G]$. From equation (1), this matrix is given by

$$[G] = \begin{bmatrix} 0 & 2\beta_0 - \frac{3\gamma}{16} (\theta - \phi) \\ -2\beta_0 + \frac{3\gamma}{16} (\theta - \phi) & 0 \end{bmatrix} \quad (17)$$

where β_0 is the equilibrium coning angle. To the order considered in this paper, β_0 is

$$\beta_0 = \frac{p^2 - 1}{p^2} \beta_{pc} + \frac{\gamma}{8p^2} (\theta - \phi) \quad (18)$$

where β_{pc} is the blade precone. The β_0 portion of [G] is the gyroscopic Coriolis term due to rotational effects. The $(3\gamma/16)(\theta - \phi)$ portion of [G] is an apparent Coriolis term due to the conservative portion of the aerodynamic coupling.

The matrix [G] is antisymmetric and is, therefore, unaffected by coordinate transformations. Thus, [G] will alter the response even when the model axis is aligned with the $(\theta + \phi)/2$ axis. In terms of the instability mechanism described earlier, the blade motion is least stable when [G] = 0 and the coupling is minimized. From equations (17) and (18), this condition occurs when

$$\left. \begin{aligned} \beta_0 &= \frac{3}{32} \gamma (\theta - \phi) \\ \beta_{pc} &= \frac{\gamma}{8} (\theta - \phi) \frac{3p^2 - 4}{4(p^2 - 1)} \end{aligned} \right\} \quad (19)$$

For $\beta_{pc} = 0$, the minimum damping condition becomes $p = \sqrt{4/3}$ for all values of $(\theta - \phi)$. This same result was obtained in reference 1 using a different method. Thus, the least stable condition occurs when all Coriolis coupling is eliminated by the equilibrium coning.

The quantitative increase in damping when β_{pc} is not given by equation (19) can be found from the contribution of [G] to the mode shape ϕ_β , equation (4b).

$$\phi_\beta \Big|_{\text{due to [G]}} = \omega_\zeta \frac{\left[2\beta_0 - \frac{3\gamma}{16} (\theta - \phi) \right]}{(\omega_\zeta^2 - p^2)^2 + \left(\frac{\gamma}{8} \omega_\zeta \right)^2} \left[-\frac{\gamma}{8} \omega_\zeta + i(\omega_\zeta^2 - p^2) \right] \quad (20)$$

The contribution to ϕ_β given in equation (20) may be added directly to the contribution in equation (15) because β_0 , θ , and ϕ are small quantities. Substitution of the combined mode into equation (9b) gives the contribution of the Coriolis terms to the blade damping.

$$-\frac{16}{\gamma} \eta \Big|_{\text{due to [G]}} = + \frac{\omega_\zeta^2 \left[2\beta_0 - \frac{3\gamma}{16} (\theta - \phi) \right]^2}{(\omega_\zeta^2 - p^2)^2 + \left(\frac{\gamma}{8} \omega_\zeta \right)^2} \quad (21)$$

Of course this damping is only indirectly due to the conservative Coriolis forces and is a direct result of the flap damping. An interesting fact is that the damping due to [G] and the damping due to [K] are uncoupled. This is because the mode shape contributions of [K] and [G] are orthogonal. Each effect provides positive damping independent of the other, and neither of the terms can provide negative damping to cancel the effect of the other.

As in the case with elastic coupling, there is a range of Coriolis coupling for which the mode shape is so far from the $(\theta + \phi)/2$ axis that no instability is possible. From equations (16) and (21), this condition is

$$\left| \frac{16}{\gamma} \beta_0 - \frac{3}{2} (\theta - \phi) \right| > \frac{\theta - \phi}{2} \sqrt{1 + \frac{(\omega_\zeta^2 - p^2)^2}{\left(\frac{\gamma}{8} \omega_\zeta\right)^2}} \quad (22a)$$

For the special cases $\Delta = 0$ or $\omega_\zeta = p$, a more restrictive criterion is obtained.

$$\left| \frac{16}{\gamma} \beta_0 - \frac{3}{2} (\theta - \phi) \right| > \frac{\theta - \phi}{2} \quad (22b)$$

This formula can be written in terms of β_{pc} and p^2 from equation (18). Thus, for $p^2 > 1$, no instability is possible for

$$\left. \begin{aligned} \beta_{pc} &> \frac{\gamma}{8} (\theta - \phi) \\ \beta_{pc} &< \frac{\gamma}{16} (\theta - \phi) \frac{p^2 - 2}{p^2 - 1} \end{aligned} \right\} \quad (23)$$

Figure 6 shows the regions for which no instabilities are possible when $\Delta(\omega_\zeta^2 - p^2) = 0$. Also shown is the contour of the least stable condition, equation (19). When $\Delta(\omega_\zeta^2 - p^2) \neq 0$, the area of possible instabilities is slightly enlarged. Thus, the Coriolis matrix [G] is a stabilizing influence. The least stable condition is [G] = 0 and, for sufficiently large [G], no instabilities are possible.

The damping expression, including elastic and Coriolis coupling terms, can be written from equations (16) and (21).

$$\eta = -\frac{\gamma}{16} \left[2 \frac{C_{d0}}{a} - \frac{(\theta - \phi)^2}{4} \right] - \frac{\gamma}{16} \frac{(\omega_\zeta^2 - p^2)^2 \left(\frac{\Delta}{\omega_\zeta^2 - p^2} - \frac{\theta + \phi}{2} \right)^2 + \left(\frac{\gamma}{8} \omega_\zeta \right)^2 \left[\frac{16}{\gamma} \beta_0 - \frac{3}{2} (\theta - \phi) \right]^2}{(\omega_\zeta^2 - p^2)^2 + \left(\frac{\gamma}{8} \omega_\zeta \right)^2} \quad (24)$$

Equation (24) shows that curves of constant damping form ellipses in the $(16/\gamma)\beta_0, \Delta/(\omega_\zeta^2 - p^2)$ plane. For example, the family of ellipses having only profile drag damping, $\eta = -(\gamma/8)(C_{d0}/a)$, is illustrated in figure 7. The thickness ratio of each ellipse in this family is $(\gamma/8)\omega_\zeta/(\omega_\zeta^2 - p^2)$. Every ellipse also passes through the same four points,

$$\frac{16}{\gamma} \beta_0 = (\theta - \phi), 2(\theta - \phi)$$

$$\delta_m = \frac{\Delta}{\omega_\zeta^2 - p^2} = \phi, \theta$$

and no ellipse contains any of the four shaded areas. Thus, the area outside of the unshaded cross is always stable.

PITCH-FLAP AND PITCH-LAG COUPLING

Pitch-flap coupling θ_β and pitch-lag coupling θ_ζ are parameters that describe the pitching motion of the rotor blade due to flap or lead-lag deflections.

$$\delta\theta = \theta_\beta\beta + \theta_\zeta\zeta \quad (25)$$

These parameters are defined so that positive flap (upward) and positive lead-lag (forward) motion produce positive pitch. Their effect on the flap-lag equations is seen in the stiffness matrix from equation (1)

$$[K] = \begin{bmatrix} p^2 - \frac{\gamma}{8} \theta_\beta & \Delta - \frac{\gamma}{8} \theta_\zeta \\ - & - \\ \Delta - \frac{\gamma}{8} \theta_\beta & \omega_\zeta^2 \end{bmatrix} \quad (26)$$

where $\bar{\theta}_\beta \equiv [\theta + (8/\gamma)(\beta_0 - \beta_{pc})\Delta\theta]\theta_\beta$. The effect of θ_β on the K_{11} term is usually treated by defining an equivalent flapping frequency

$$\bar{p}^2 \equiv p^2 - \frac{\gamma}{8} \theta_\beta$$

It should be noted, however, that the equilibrium formula, equation (18), is still valid in its present form in terms of p^2 and $(\theta - \phi)$. It may be rewritten, however, in terms of \bar{p}^2 and $(\theta_0 - \phi)$.

$$\beta_o = \frac{\bar{p}^2 - 1}{\bar{p}^2} \beta_{pc} + \frac{\gamma}{8\bar{p}^2} (\theta_o - \phi)$$

The coefficients in equation (1) must be expressed in terms of the total equilibrium pitch angle, $\theta = \theta_o + \theta_\beta(\beta_o - \beta_{pc})$. Thus, pitch-flap coupling affects the blade dynamics by changing the flapping frequency and the blade equilibrium.

Another effect of θ_β and θ_ζ is the coupling produced in the off-diagonal terms K_{12} and K_{21} . First, the pitch-lag coupling θ_ζ changes the mode shape by altering K_{12} , equation (4b). This effect can be included in the analysis by replacing Δ with $\Delta - (\gamma/8)\theta_\zeta$ in equation (24). A second effect of θ_ζ and θ_β is that they produce an asymmetric or nonconservative stiffness matrix. The energy dissipated or added by this asymmetry can be approximated by integrating the dot product of force and distance around a closed path, figure 3. The integration yields

$$\begin{aligned} \text{Energy dissipated} &= \oint (F_1 dx_1 + F_2 dx_2) \\ &= \oint (K_{11}x_1 dx_1 + K_{22}x_2 dx_2 + K_{12}x_2 dx_1 + K_{21}x_1 dx_2) \\ &= \oint \left[K_{11} d\left(\frac{1}{2} x_1^2\right) + K_{22} d\left(\frac{1}{2} x_2^2\right) + K_{12}(x_2 dx_1) + K_{21}(x_1 dx_2) \right] \end{aligned}$$

The energy dissipated can be evaluated from the following relations: (1) the integral around a closed contour of a perfect differential is zero, (2) the integration of $x_1 dx_2$ is the area enclosed within the contour, and (3) the integration of $x_2 dx_1$ is the negative of the enclosed area.

$$\text{Energy dissipated} = (K_{21} - K_{12}) (\text{enclosed area}) \quad (27)$$

The area is taken as positive for integration in a clockwise direction. Thus, the nonconservative or antisymmetric portion of $[K]$ may either dissipate or add energy.

For the particular case of flap-lag dynamics, the enclosed area is approximated by the area of the ellipse of motion $\rho\pi$; and the antisymmetric stiffness term is $K_{21} - K_{12} = (\gamma/8)(\bar{\theta}_\beta + \theta_\zeta)$. Thus, the damping contribution due to the nonconservative terms is

$$\eta|_{\text{nonconservative stiffness}} = -\frac{\text{Energy dissipated}}{2\pi\omega_\zeta} = -\frac{\gamma}{16} \frac{\rho}{\omega_\zeta} (\bar{\theta}_\beta + \theta_\zeta) \quad (28)$$

Thus, energy is either added or dissipated depending on the sign of $\bar{\theta}_\beta + \theta_\zeta$ and the sense of the motion ($\rho > 0$ clockwise, $\rho < 0$ counterclockwise). taking $\Delta = \Delta - (\gamma/8)\omega_\zeta$ in equations (24) and (4b), and adding the nonconservative stiffness contribution from equation (28), one obtains the complete expression for lead-lag damping.

$$-\frac{16}{\gamma} \eta = \left[2 \frac{C_{d0}}{a} - \frac{(\theta - \phi)^2}{2} \right] + \frac{\left[\Delta - \frac{\theta + \phi}{2} (\omega_\zeta^2 - \bar{p}^2) \right]^2 + \omega_\zeta^2 \left[2\beta_0 - \frac{3\gamma}{16} (\theta - \phi) \right]^2}{(\omega_\zeta^2 - \bar{p}^2)^2 \left(\frac{\gamma}{8} \omega_\zeta \right)^2}$$

$$+ \frac{\frac{\gamma}{8} (\bar{\theta}_\beta - \theta_\zeta) \left[\Delta - \frac{\theta + \phi}{2} (\omega_\zeta^2 - \bar{p}^2) \right] + (\bar{\theta}_\beta + \theta_\zeta) (\omega_\zeta^2 - \bar{p}^2) \left[2\beta_0 - \frac{3\gamma}{16} (\theta - \phi) \right] - \left(\frac{\gamma}{8} \right)^2 \bar{\theta}_\beta \theta_\zeta}{(\omega_\zeta^2 - \bar{p}^2)^2 + \left(\frac{\gamma}{8} \omega_\zeta \right)^2}$$

(29)

The second line of equation (29) represents the effect of pitch-flap and pitch-lag coupling on blade damping.

The effect of pitch-flap coupling is entirely due to the nonconservative terms. Thus, for clockwise motion in the x_1, x_2 plane, positive $\bar{\theta}_\beta$ is stabilizing. Equations (15) and (20) show that the motion is clockwise when $\rho > 0$ or

$$(\omega_\zeta^2 - \bar{p}^2) \left\{ \left[\frac{\Delta - \frac{\gamma}{8} \theta_\zeta}{\omega_\zeta^2 - \bar{p}^2} - \frac{\theta + \phi}{2} \right] + \left[\frac{16}{\gamma} \beta_0 - \frac{3}{2} (\theta - \phi) \right] \right\} > 0 \quad (30)$$

which agrees with equation (29). This effect is illustrated in figure 9. There is a straight line that divides the $\bar{\delta}_m, (16/\gamma)\beta_0$ plane into two regions in which blade motions are either clockwise or counterclockwise. Along this straight line boundary $\rho = 0$ and blade motions enclose no area. Thus, on this boundary pitch-flap coupling has no effect. Of interest is the fact that the minimum damping point with $\theta_\beta = \theta_\zeta = 0$ is on this boundary and also represents a condition unaffected by θ_β .

For pitch-lag coupling, there are nonconservative stiffness terms and elastic coupling terms that affect the damping. When both effects are included, the boundary between stabilizing and destabilizing regions is a straight line in the $\bar{\delta}_m, (16/\gamma)\beta_0$ plane. This effect is illustrated in figure 10 which gives the total effect of θ_ζ on blade damping except for the $\theta_\zeta \theta_\beta$ coupling effect already treated in equation (30). The boundary between the stabilizing and destabilizing regions is perpendicular to the $\bar{\theta}_\beta$ boundary in figure 9 and passes through the same minimum damping point. Thus, at the condition of minimum damping with $\theta_\beta = \theta_\zeta = 0$, there is no effect of θ_β or θ_ζ alone, although there is a coupling effect if θ_β and θ_ζ are included together. There are, therefore, three factors that can change the effect of

θ_β or θ_ζ from stabilizing to destabilizing or vice versa: (1) the sign of $\bar{\theta}_\beta$ or θ_ζ , (2) the sign of $(\omega_\zeta^2 - \bar{p}^2)$, and (3) the region (i.e., half-plane) in which $(16/\gamma)\beta_0$ and δ_m (or $\bar{\delta}_m$) lie.

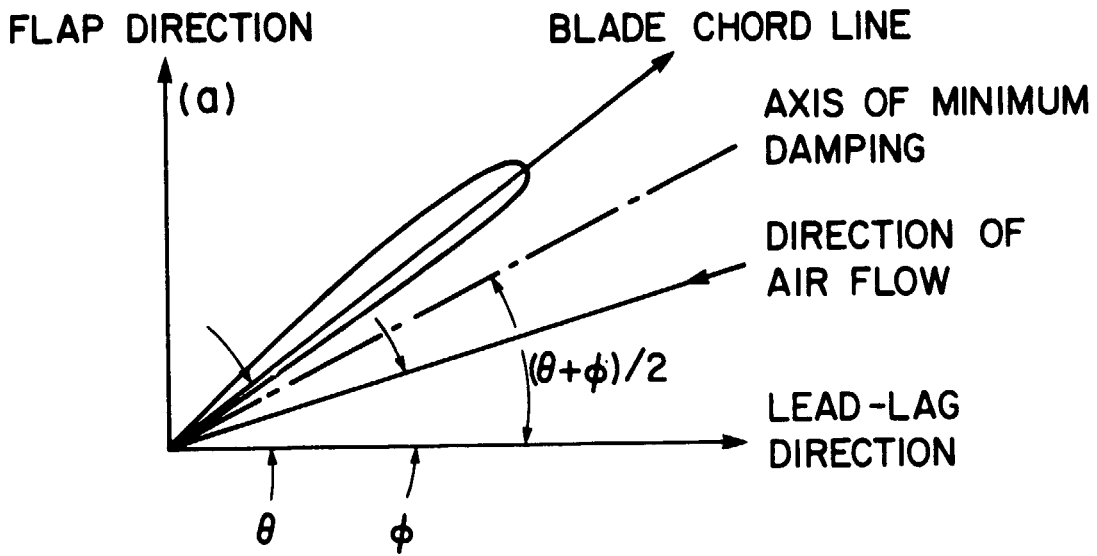
CONCLUSIONS

The following conclusions may be drawn from this analysis.

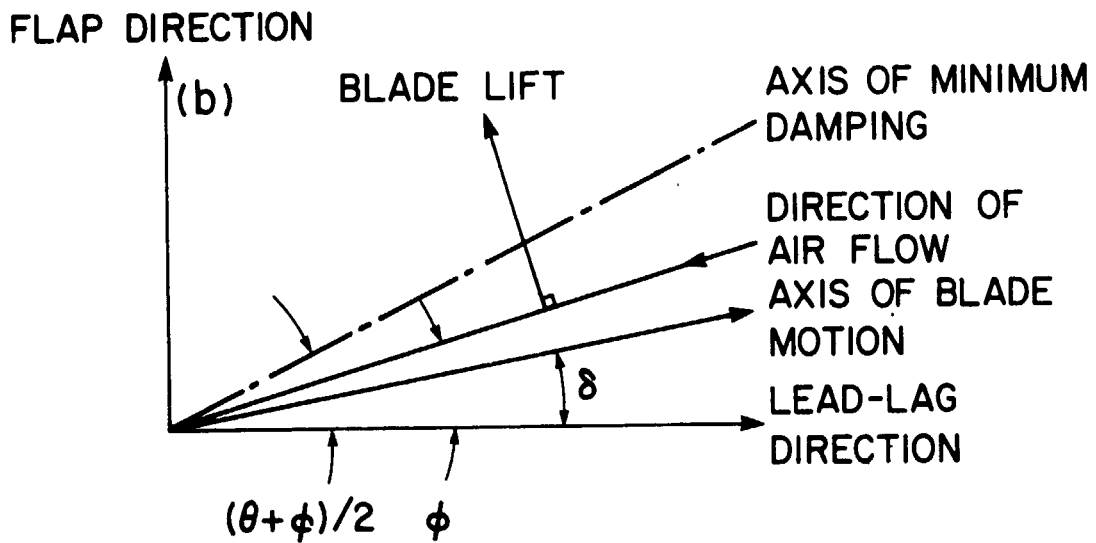
1. The destabilizing effect of aerodynamic forces that can occur when $(\theta - \phi) > 2\sqrt{2(C_{d0}/a)}$ is maximum when the blade motion is in a straight line along the $(\theta + \phi)/2$ axis.
2. Coriolis and elastic coupling can move the mode shape with respect to the $(\theta + \phi)/2$ axis and thereby influence the blade stability.
3. The least stable condition occurs when the Coriolis terms are zero and when the elastic coupling terms align the rotating mode shape in a vacuum with the $(\theta + \phi)/2$ axis.
4. Pitch-lag coupling produces a change in the equivalent elastic axis, and pitch-flap and pitch-lag coupling introduce nonconservative stiffness terms that stabilize or destabilize the blade motion depending upon whether the motion is clockwise or counterclockwise.

REFERENCES

1. Ormiston, R. A. and Hodges, D. H.: Linear Flap-Lag Dynamics of Hingeless Helicopter Rotor Blades in Hover. J. American Helicopter Soc., vol. 17, no. 2, April 1972.
2. Zajac, E. E.: The Kelvin-Tait-Chetaev Theorem and Extensions. J. Astronaut. Sci., vol. 11, no. 2, Summer, 1964, pp. 46-49.



(a) Motion geometry.



(b) Force geometry.

Figure 1.- Geometry of blade motion and aerodynamic force.

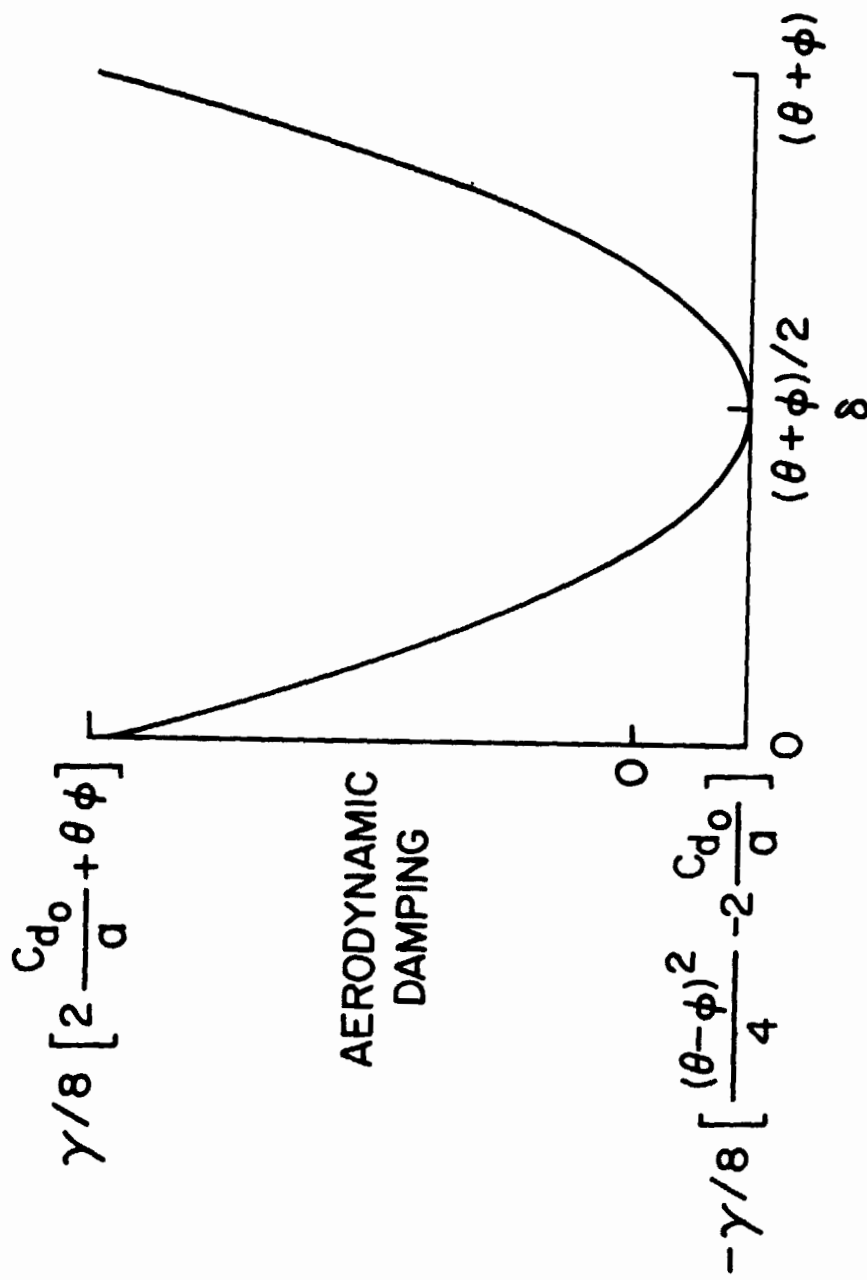


Figure 2.- Aerodynamic damping coefficient for motion in δ direction.

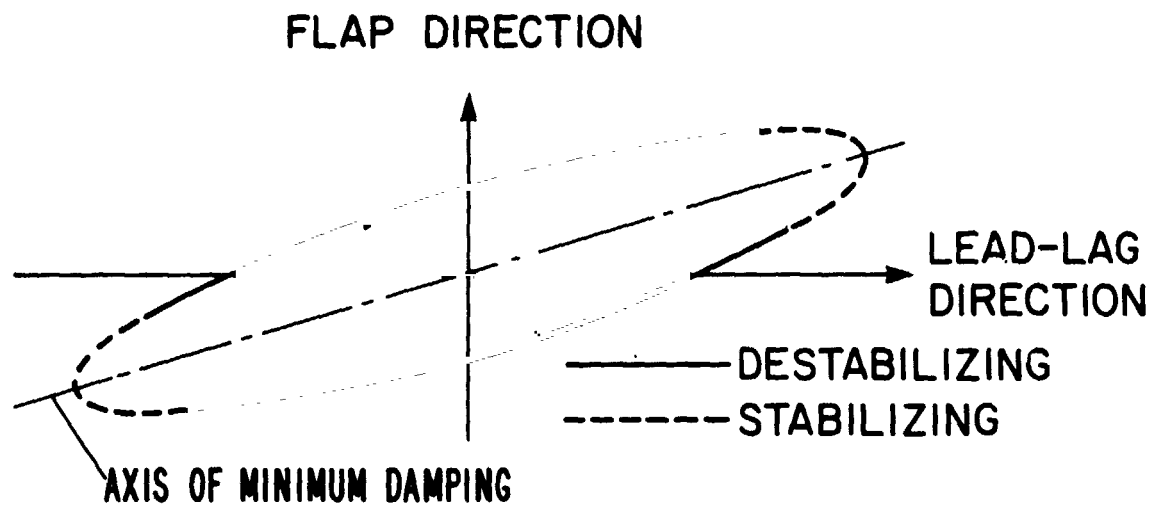


Figure 3.- Elliptical blade motions.

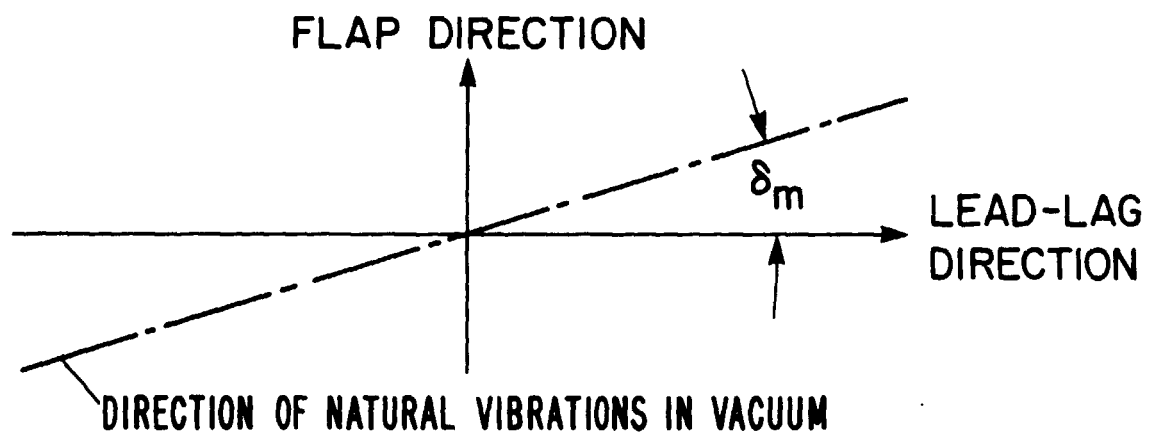


Figure 4.- Rotating mode shape in vacuum.

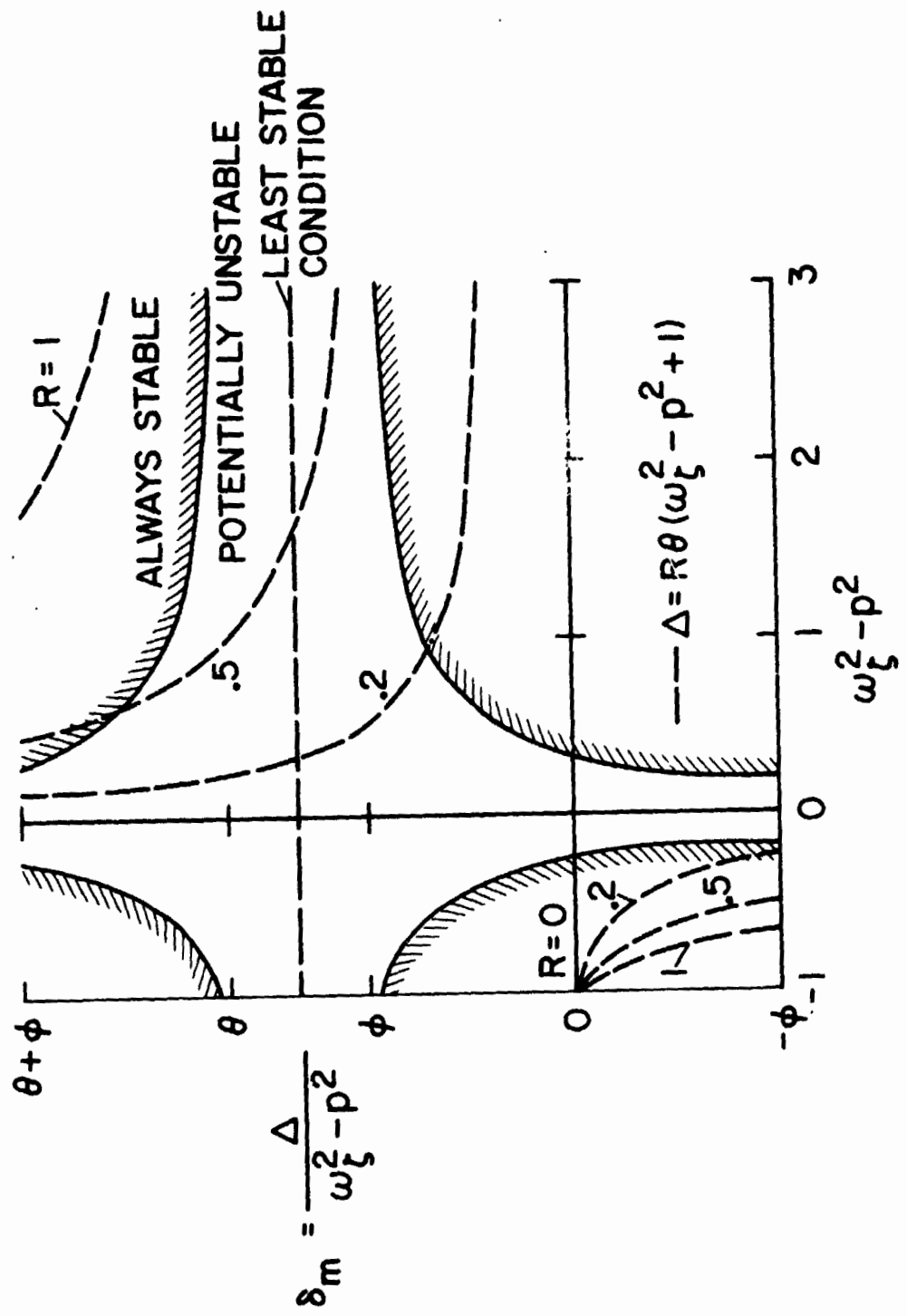


Figure 5.- Effect of elastic coupling on regions of potentially unstable motion, $\gamma = 8$, $p = \sqrt{4/3}$. No pitch coupling.

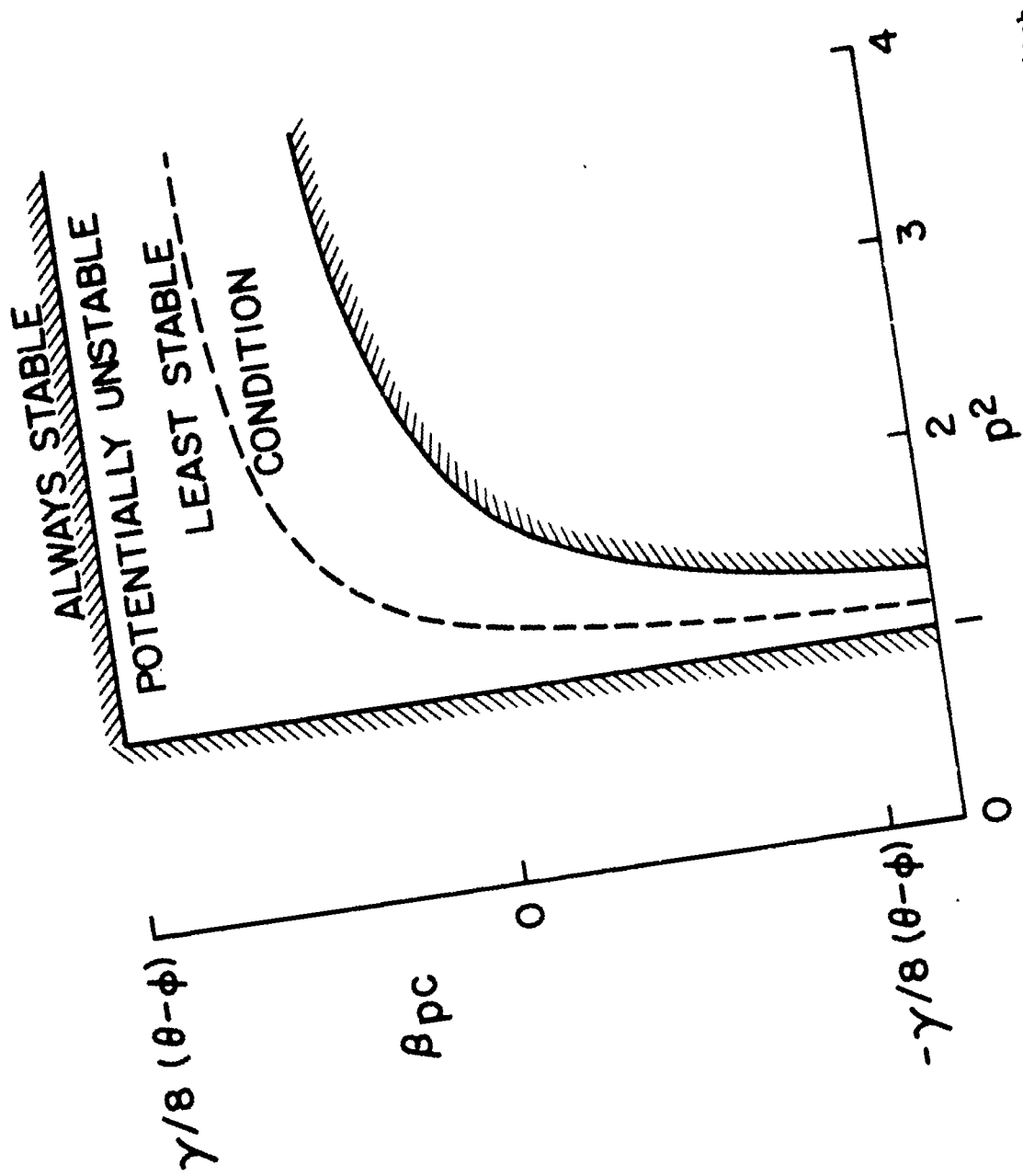
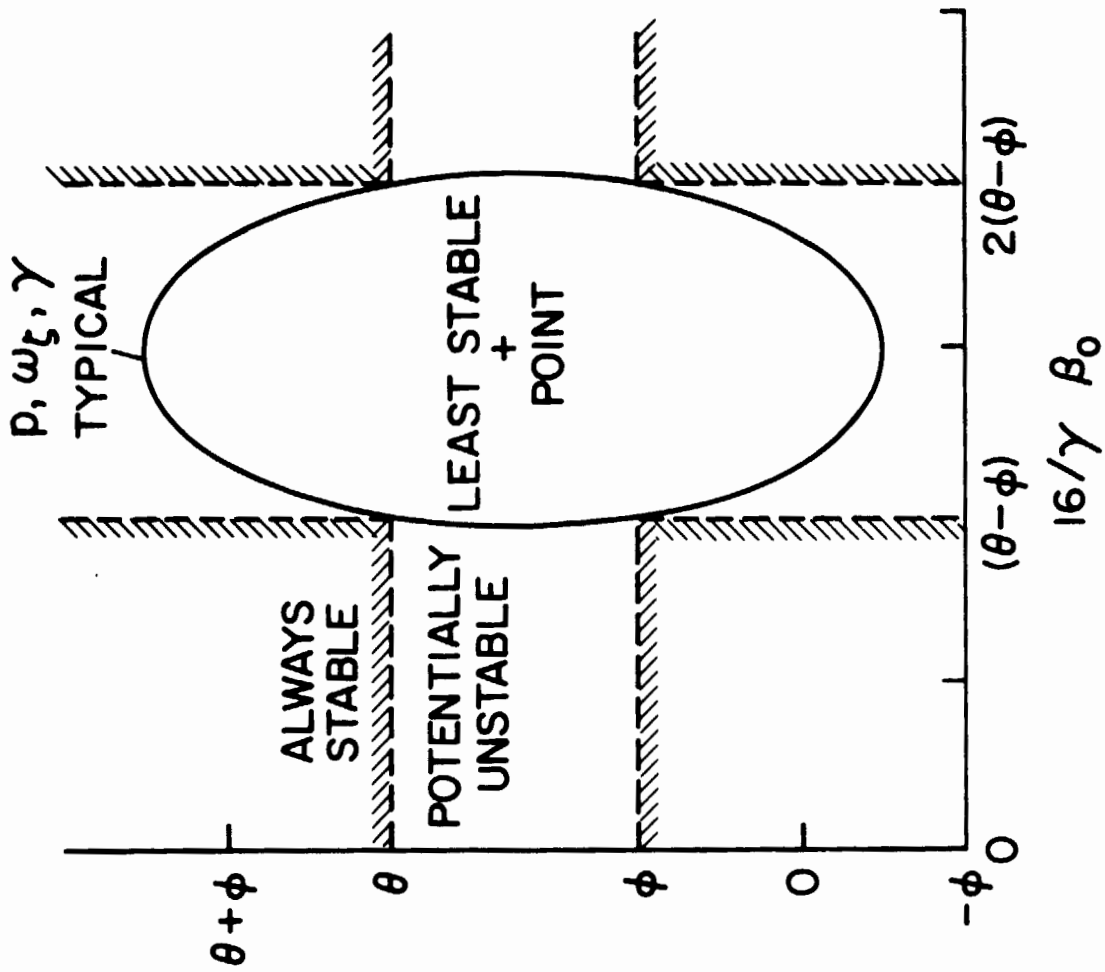


Figure 6.- Effect of Coriolis coupling when $\Delta(\omega_c^2 - p^2) = 0$. No pitch coupling.



$$\delta_m = \frac{\Delta}{\omega_\zeta^2 - p^2}$$

Figure 7.- Ellipse of constant damping $\eta = -(\gamma/8)(C_{D0}/a)$, and regions of potentially unstable motion. No pitch coupling.

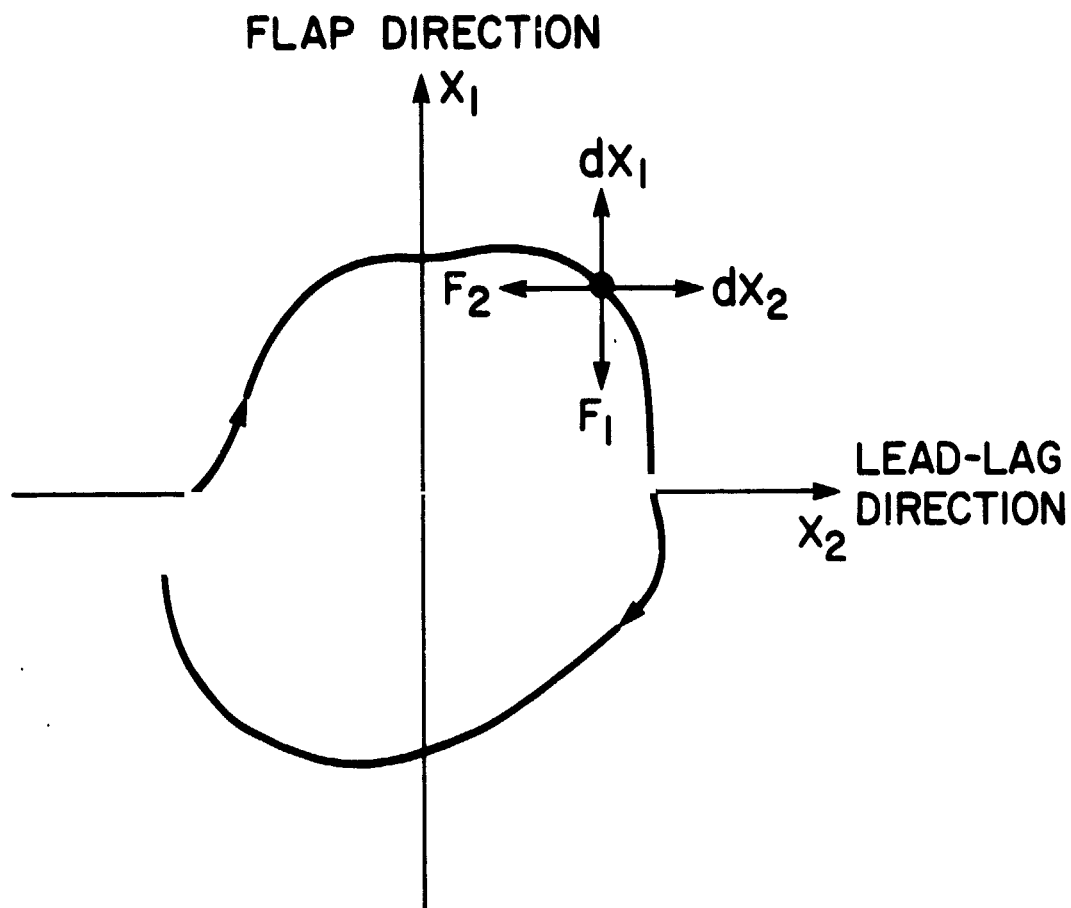


Figure 8.- Energy dissipated for motion around a closed contour.

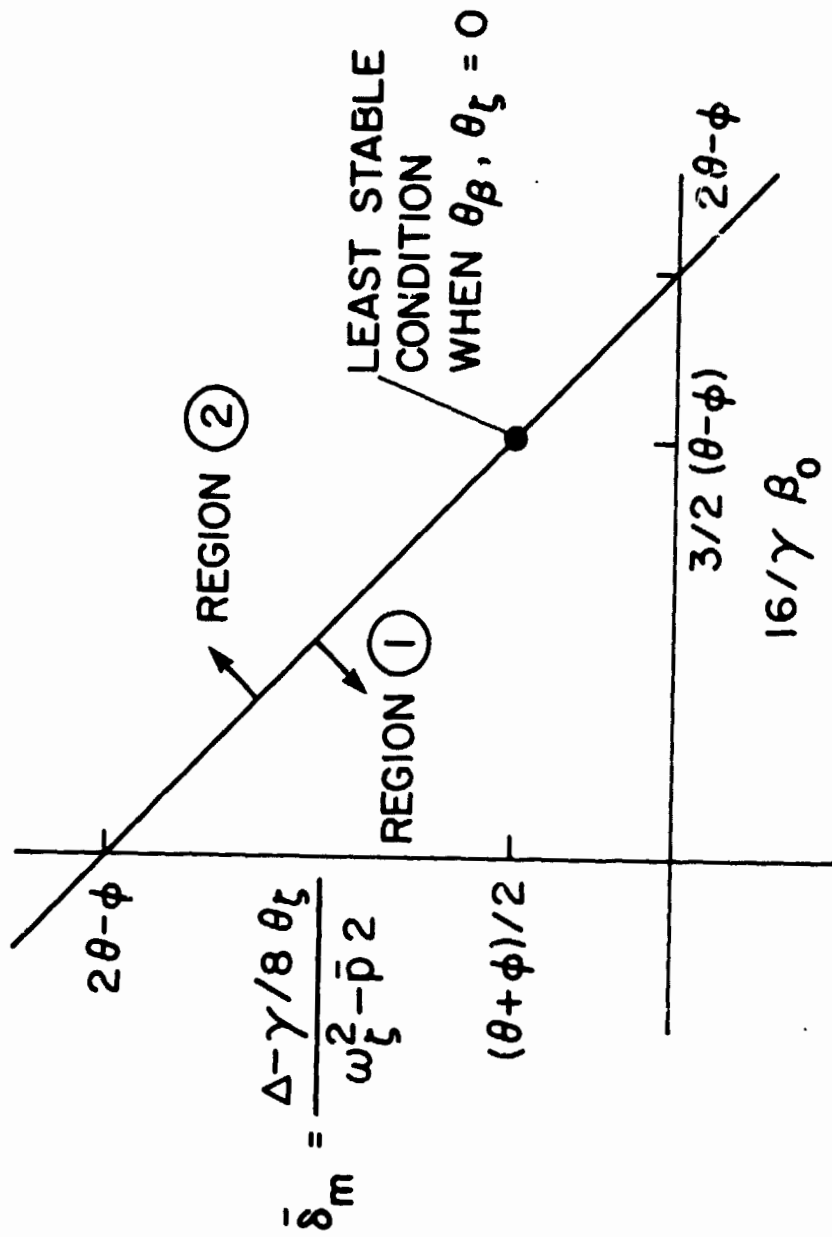


Figure 9.- Effect of pitch-flap coupling. Blade motion is destabilized in region $\begin{cases} (1) & \text{when } (\omega_\zeta^2 - \bar{p}^2)\bar{\theta}_\beta > 0 \\ (2) & \text{when } (\omega_\zeta^2 - \bar{p}^2)\bar{\theta}_\beta < 0 \end{cases}$.

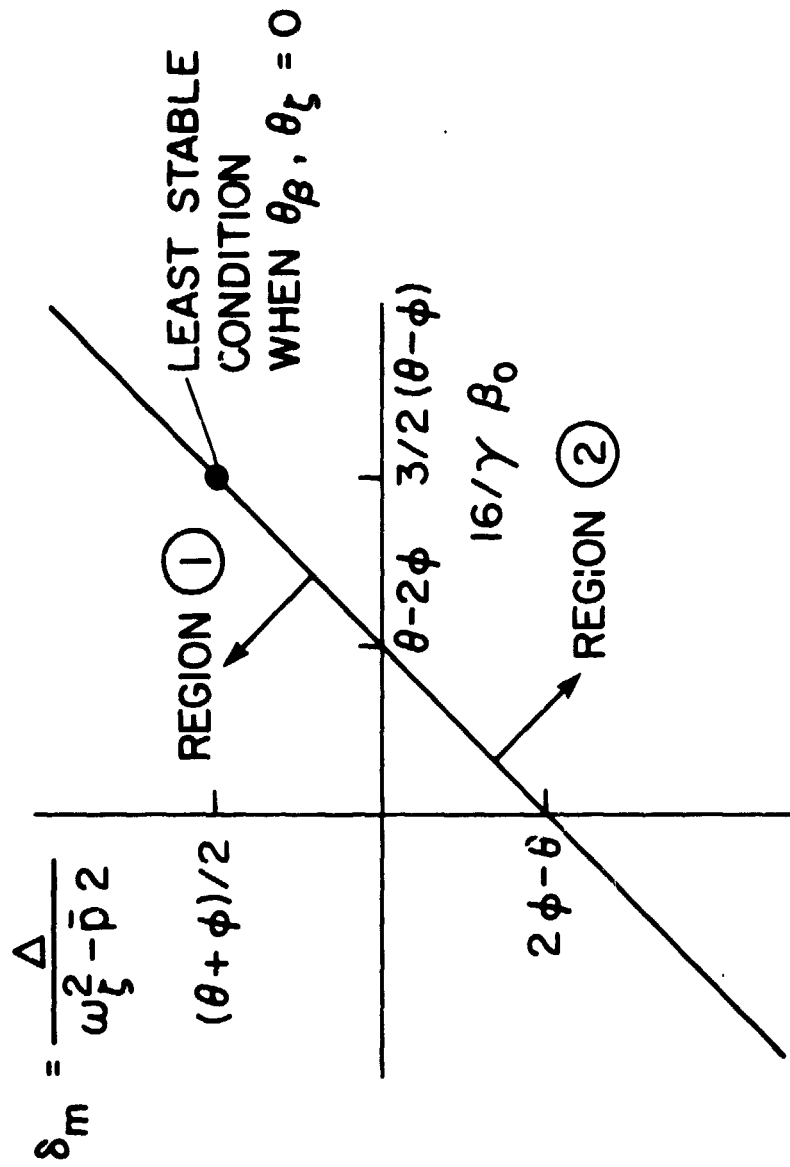


Figure 10.- Effect of pitch-lag coupling. Blade motion is destabilized in region (1) when $(\omega_z^2 - \bar{p}^2)\theta_z > 0$ and in region (2) when $(\omega_z^2 - \bar{p}^2)\theta_z < 0$.